A SELECTED COMPARISON FROM ATC TEST: INDUSTRY PROGRESS FROM 2005 TO PRESENT DAY

John McMahon, Russell Brush, and Brian Standing
Celestica Inc.
Toronto, ON, Canada
jmcmahon@celestica.com

ABSTRACT
Accelerated thermal cycling (ATC) is the accepted test methodology for characterizing the expected service life of electronic components. When combined with vibration, shock and bend testing it can provide a reasonable confidence that the material under test will perform robustly in field service. Since the year 2005 the team has conducted ATC testing on over 500 lots of components. Looking back at some of the early work and how those assembly lots would compare to current industry expectations provides some real insight to the progress made by the industry.

Package technology has progressed significantly as have process materials and chemistry. There are specific component categories where comparisons are easier to make. Ceramic ball grid array (CBGA) components are one such case.

This paper compares assembly and test of various 1.0 mm pitch CBGAs conducted between 2005 and 2014 and ranging from 32.5 x 32.5 mm and 937 IO to 55 x 55 mm and 2892 IO. Assembly yields and processes are compared as well as ATC test results. Weibull distributions and parameters are provided along with selected destructive failure analysis and discussion of the mechanisms.

Key words: Accelerated thermal cycling, Reliability testing, Ceramic components, Weibull analysis

INTRODUCTION
In 2005 there was a significant level of industry concern over the performance of Pb-free SAC based solders. Many investigators were mounting individual component comparison studies which were intended to define the difference in accelerated thermal cycling (ATC) performance between SAC alloys and eutectic Sn37Pb solders. In fact, many investigators were proposing SAC387 as a more reliable option than the already common SAC305. The authors were part of a much larger team that conducted a wide ranging experiment based around 10 surface mount component types and three pin through hole component types intended to define the effects of surface finish, peak temperature, reflow environment and alloy across multiple board thicknesses and ATC test conditions [1]. Reworked components were included in all of the technology types. All were daisy chained parts, were present multiple times on the test vehicle and multiple times per side if they were placed on both bottom and top. This test program yielded a tremendous amount of data and provided the basis for much of the work that has been accomplished by that team in the subsequent years.

In this work we are primarily interested in the assembly and thermal stressing of a single component included in that study. The CBGA937 was a co-fired ceramic component with a 31 x 31 array of 1.0 mm pitch solder spheres and 6 depopulated sites at each corner. This particular device exhibited early failures and a relatively short characteristic life under cycling stress. The results conflicted with some earlier testing and needed to be validated by physical failure analysis, but upon confirmation convinced the authors that there was very little likelihood that ceramic area array components would be viable under the terms of the RoHS legislation even in controlled server room and corner office environments.

While it is true that the higher stresses generated by ceramic components continue to be an issue in Pb-free electronic assembly service life, it is generally driven by low stand off ceramic devices such as oscillators and large capacitors which tend to be the first point of failure on a wide range of server room products. It is also evident that these Alumina based ceramic devices have not been widely applied as the industry moved forward with the larger BGA based devices and thicker boards required to accomplish the increased data rates and capability we see in server room products today.

However, there have been significant advances in base materials and attachment technology that insure that ceramic components are still a viable option for server room applications. Initial publication of edge bond material performance was published by Song [2] and related to supporting BGA style mezzanine connectors. The authors believe that these improvements are significant enough that they should be evaluated for application in other industry sectors and service environments.

This work documents the progress in enhancing solder fatigue chamber life in CBGA devices by examining four specific projects which were representative of the leading edge of the industry at the time they were undertaken. All of these enhancements have now been implemented into mass production programs but some have not been widely accepted.

Specifically we compare projects to demonstrate the benefit to ATC performance and therefore field service life of three material/process improvements.

- Low Temperature Co-fired Ceramic (LTCC) substrates
- Mechanical stand offs at the corner of large devices
- Reworkable edge bonding material

Where possible direct project comparisons are made using the same alloy as well as, board material, thicknesses and stack up. However the nature of the industry and this type of qualification work dictates that package sizes are always increasing with time.

ASSEMBLY PROCESSES

COMPONENT A

Component A was incorporated into the RIA3 Test Vehicle (TV). The RIA3 TV was 8" x 10" in size, 0.093" thick with 10 inner layers of 0.5 oz. copper and surface layers 1 and 12 plated up to 1 oz. copper. The stack-up featured 8 signal layers and 4 ground plane layers, arranged as follows: SSGSSGGSSGSS. The RIA3 test vehicles were procured in a variety of different surface finishes. These included conventional OSP, Immersion Silver (8-12 µin), Immersion Tin (40 µin), Electrolytic Nickel (200-800 µin)/Gold (3-15 µin) and ENIG ((Electroless Nickel (120-240 µin) and Immersion Gold (2-5 µin)).

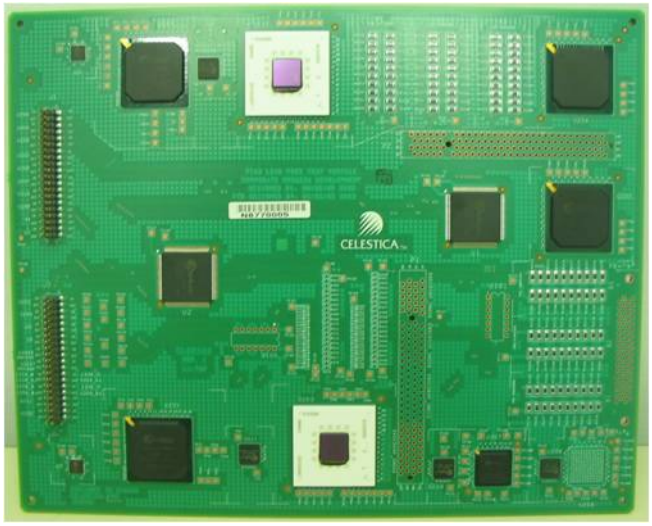

Figure 1: Comp A (Ria 3) test Vehicle

The white CBGA devices visible in Figure 1 have a 31 x 31 full array of solder spheres on a 1.0 mm pitch and had 6 locations depopulated in each corner for a total of 937 IO. The component side pad was 0.028 inches (710 µm), the board side solder pad was 0.024 inches (610 µm) and the stencil aperture was 0.022 inches (560 µm) in a 0.005"(125 µm) foil. The target range for the paste deposit was between 1500 and 2500 cubic mils and the process achieved an average of 1828 cubic mils.

The profile for the lots under discussion generated the parameters listed in Table 1 for the CBGA device at U203

Table 1: Comp A – Reflow Parameters

U203	Peak T.(°C)	TA-217(sec)
Center SJ	234	75
Corner SJ	241	76

It should be noted that both primary attach (PA) and forced rework (FR) lots were included and that this TV was subsequently processed through wave solder attachment in an exclusion fixture prior to thermal cycling. This is the only TV in the group that experienced this particular thermal excursion.

COMPONENT B

Component B was assembled for an independent second level reliability assessment and assembled again at a later date to provide information on reworkable edge bond material. Forty-four (44) (33 PA devices and 11 FR) devices were assembled onto 0.125 inch (3.175 mm) thick test vehicle boards in a symmetric square pattern of 47.5 mm footprints. The TV was fabricated using a filled Phenolic cured FR4 epoxy with a T_g of 180°C and a T_d of 240°C. This TV had a symmetric 16 layer stack up of plane and signal layers all in 0.5 oz. copper. The footprint was a full array of 46 x 46 with a single ball depopulated at the A1 position. There were either 5 or 6 solder mask defined (SMD) pads at each corner. The component is displayed in Figure 2 and the pad and solder mask opening dimensions are listed in Table 2.

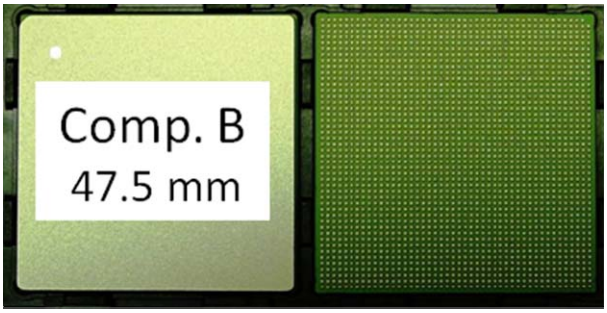

Figure 2: Component B

Table 2: Comp B – PWB Pad Sizes

Comp B - PWB	NSMD	SMD
Pad Diameter	24 mil	26 mil
Solder Mask Opening	28 mil	24 mil

The stencil was a standard laser cut 0.006 inch (150 µm) foil with 0.024 inch (610 µm) round apertures. The paste was a SAC305 alloy in a type 3 powder and an 89% metal load combined with a standard ROL0 flux vehicle. The average paste volumes by component location are available in Table 3.

Table 3: Comp B - Paste Measurement

Ref Des.	Avg. Vol. (mils^3)	Avg. Ht. (mils)
U1	2906.7	7.69
U2	2897.3	7.69
U3	2871.5	7.88
U4	2891.1	7.74

The boards were reflowed in twelve zone convection oven with an additional 4 cooling zones. The resulting reflow parameters are tabulated in
Table 4.

Table 4: Comp B – PA Reflow Parameters

Location	Peak T.(°C)	TA-217(sec)
Center SJ	230.1	76
Corner SJ	235.1	86
FR4	248.4	115

Forced rework was accomplished using a SAC305 alloy in a Type 5 powder and an 81% metal load combined with a standard ROL0 flux vehicle. The rather different reflow parameters generated by hot gas rework equipment are documented in Table 5.

Table 5: Comp B - FR Reflow Parameters

Component	Peak T. (°C)	TA 217 °C (sec)
Center SJ	252	137
Corner 1 SJ	232	67
Corner 2 SJ	244	126

Figure 3: Comp B with Edge Bond

At a later date 24 Component B devices, 23 PA and 1 FR were independently assembled onto the same test vehicle and then reinforced with a high viscosity reworkable edge bond material in the pattern shown in Figure 3. The edge bond material was cured at 125 °C for 25 minutes.

COMPONENT C

Component C was assembled for an independent second level reliability assessment. The TV was intended to evaluate the reliability of a 50 mm, 1.0 mm pitch, 2303 I/O BGA package (48x48-1) and compare three versions which varied by lid type and attachment as well as thermal interface material (TIM) as laid out in Table 6. The test vehicle was a 16 layer 0.125 inch (3.175 mm) thick Phenolic cured FR4 epoxy with a Tg of 180°C and Td of 340°C.

There were 33 PA devices and 11 FR devices distributed over 11 TV boards for each version of the component.
All BGA pads on the board were non-solder mask defined with a pad diameter of 0.024 inches (610 µm), except for the 6 pads in each corner which were solder mask defined. The SMD areas had a pad diameter of 0.026 inches (660 µm) and a solder mask opening of 0.024 inches (610 µm). All signal and plane layers in the TV were 0.5 oz copper foil.

Table 6: Comp C - Lot Variations

Lot	Lid	TIM	Adhesive
100	AlSiC	-1-	None
200	AlSiC	-1-	-1-
300	Cu	-2-	-1-

The stencil was a 0.005 inch laser cut stainless steel foil with 0.024 inch (610 µm) diameter round apertures. The paste was a standard ROL0 flux combined with SAC305 alloy in a Type 3 powder.

Paste volumes were measured for every aperture in the study, average paste volumes and paste heights are tabulated in Table 7.

Table 7: Comp C - Paste Measurement

Location	Avg. Volume	Avg. Height
U1	2617 mil^3	6.87 mils
U2	2581 mil^3	6.77 mils
U3	2661 mil^3	6.90 mils
U4	2608 mil^3	6.78 mils

Table 8: Comp C - Reflow Parameters

Location	Peak T.(°C)	TA-217(sec)
Center SJ	233	66
Corner1 SJ	241	80
Corner2 SJ	242	81

The 33 forced rework devices were soldered using automated hot gas rework equipment and dispensing equipment to apply SAC305 paste with a Type 4 powder and a 83% metal load. The SMT reflow zone parameters for component C are displayed in Table 8.

All devices PA and FR were inspected with transmissive X-ray and no defects were detected.

COMPONENT D

Forty-four (44) devices were assembled onto 0.125 inch (3.175 mm) thick test vehicle boards in a symmetric square

pattern of 55 mm footprints. There were 11 forced rework attachments included in the lot of 44.

The screening operation was accomplished using a laser cut 0.005 inch (125 µm) foil with 22 mil (560 µm) square apertures with round corners. The solder paste was an 89% metal load SAC305 alloy in a Type 3 powder combined with a standard no-clean ROLO flux.

The footprint designed for this package utilized 0.020 inch (510 µm) diameter pads and included pads at each corner of the device outside of the ball array to provide for soldering of 0402 resistor packages under the body of the part. The placement process was preceded by dispense of a single glue dot at each corner. The footprint with paste and glue is depicted in Figure 4.

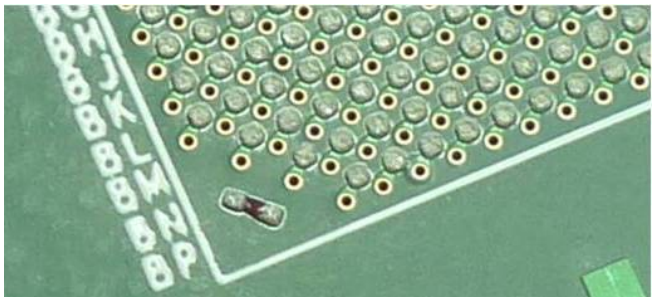

Figure 4: Comp D footprint

All boards were reflowed three times in a nitrogen environment within a 12 zone convection oven. The profile shown in Figure 5, exhibits thermal excursions for thermo-couples located in the solder joints at the center and two corners of a single device and on the surface of the FR4 near the mid-point of the board. Table 9 summarizes the key parameters. Note that for high thermal mass assemblies of this type molten time is significantly longer than Time above 217℃ due to under cooling of the solder.

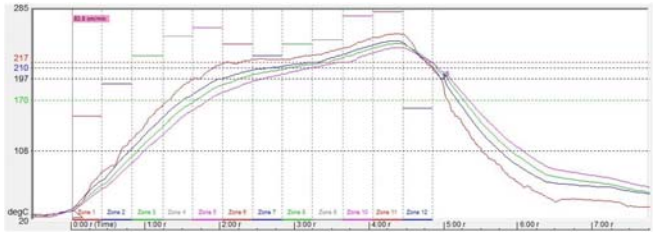

Figure 5: Comp D - Thermal Profile

Table 9: Comp D - Reflow Parameters

Location	Peak T.(℃)	TA-217(sec)
Center SJ	236	71
Corner1 SJ	241	84
Corner2 SJ	244	91
FR4	253	154

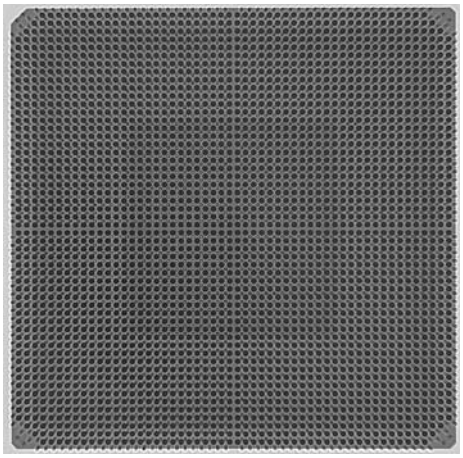

Figure 6: Comp D Transmissive Xray

All assemblies were inspected by transmissive X-ray. A typical X-ray image of a primary attached component is shown in Figure 6. All components passed X-ray inspection with all voids less than 25% of the solder ball volume and no solder-bridges.

The high viscosity reworkable edge bond material with 50% filler was dispensed in an 'L' pattern around each BGA corner leaving a small gap in the centre of each side of the component. The edge bond material was cured at 125 ℃ for 25 minutes. An image of the dispense pattern is shown in Figure 7.

Figure 7: Comp D with Edge Bond

TEST PROCESS

Test process conditions and test parameters are standardized across all of these components. Accelerated Thermal Cycling (ATC) was performed in the same make and type of chamber. The target conditions were identical and in all cases the ramp rates and dwell conditions complied with IPC9701, test condition 1.

The completed boards were supported in a 42 cubic foot single zone ATC chamber. The configuration shown in Figure 8 is typical of all of the tests. Two racks were used

to hold the boards while allowing the airflow to circulate freely.

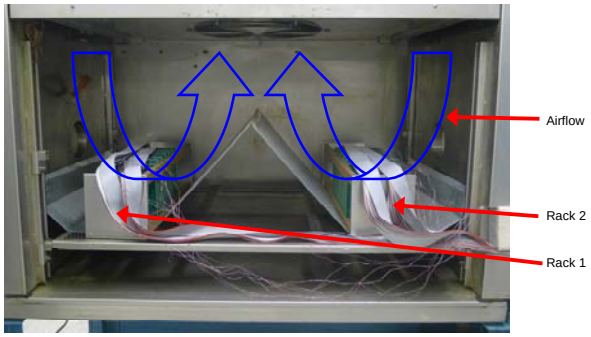

Figure 8: ATC Chamber Load

The components were fully in-situ monitored using data loggers configured for 4 wire resistance measurements. The data was collected and logged every 60 seconds. Failure was defined as five consecutive readings showing a minimum 20% resistance increase over the resistance measured during the hot dwell on the first cycle.

TEST RESULTS

COMPONENT A

This study purposely utilized a smaller component pad, solder sphere and board footprint pad size than previous work with this CBGA package. Cole [3] published that the new feature geometry was intended to produce better assembly yields by reducing bridged solder joints. The resulting solder joints are somewhat heart shaped because of the mis-match between package and board pad size. Additionally there were some issues with the fabrication of the test vehicles which were not identified prior to assembly. The solder mask was mis-registered to the extent that in some locations the solder mask overlapped the solder pad and intruded into the solder joint. This intrusion was significant enough to produce an alternate failure mode. The preliminary Weibull analysis displayed in Figure 9, shows a double slope with an inflection point typically produced by multiple independent failure modes. The lower portion of the curve is indicative of the crack path displayed in the lower photograph, where intrusion of solder mask has generated a reduced solder area and a stress concentration. The second slope is generated by the damage displayed in the upper photograph which is more typical of the normal wear out mechanism for ceramic packages.

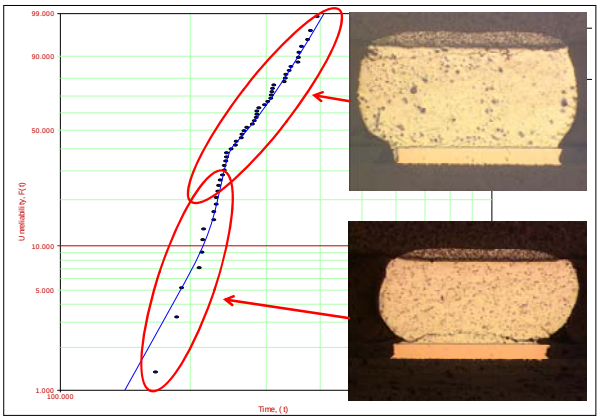

Figure 9: Comp A - Mixed Weibull Distribution

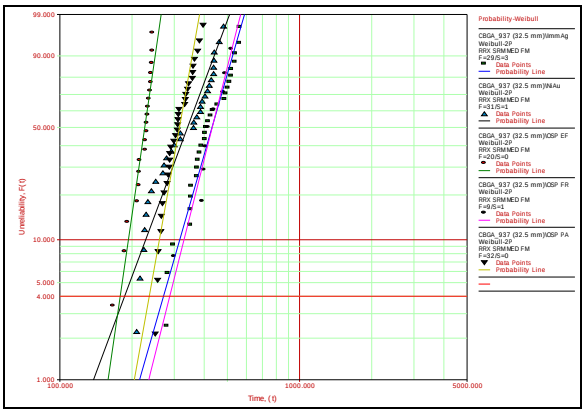

Figure 10: Comp A - Weibull Distributions

These failure modes have been separated in Figure 10 and are represented by two distinct distributions, early failure (EF) and primary attach (PA) for representative wear out mechanism. After separation the OSP lot had a calculated nominal 4% failure rate (B4%) at 235 cycles. Immersion Silver and NiAu had similar B4% values of 270 and 186 cycles respectively.

However, we should note from the 90% confidence contours (CC) displayed in Figure 11 that the surface finishes are not in their standard order and that the FR lot performed significantly better than the PA lot. These two observations indicate that the OSP PA lot has some remaining issues which have not been identified. The real wear out mechanism may produce values nearly double those recorded in this test.

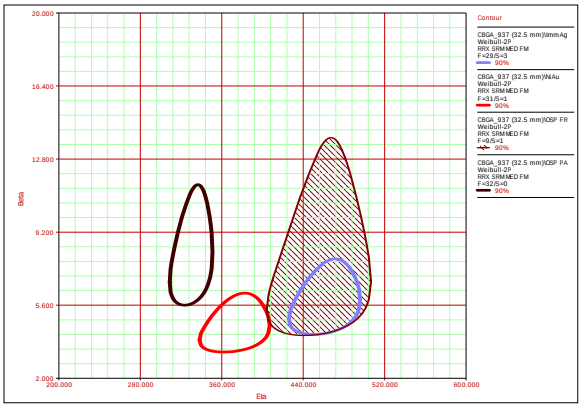

Figure 11: Comp A – 90% CC

COMPONENT B

This component test was representative of the introduction of a new LTCC substrate material with a listed coefficient of thermal expansion (CTE) over 12 ppm/℃. Butel[4] and others have published studies documenting the benefits to cycling life produced by this material. Samples removed from actual components after removal from an assembled board have been measured in house in the range of 10 ppm/℃. In either case this material represents a significantly different stress condition under thermal cycling when compared to Alumina (Al_2O_3) based ceramics. Which have CTE values near 6.4 ppm/℃.

As expected, thermal cycling of this device generated damage at and near the corners of the device at the largest distance from the neutral point (DNP). The recrystallization zone has a dish shape that is thicker near the center of the solder joint in plane and reaches outward to a circumference very close to the edge of the component side pad. The cross-sections exhibit classic SAC microstructures and the cracks propagated through the bulk solder in the recrystallized zone near the top of the solder joints. This failure mode is typical for ceramic devices. Figure 12 & Figure 13 contain images of SMD solder joint failures near the corners of the device. The ATC07-3- A46 and ATC09-4- BF46 locations were identified as perimeter chain electrical failures at 936 and 1360 cycles respectively and both were removed from the chamber for destructive analysis at 1990 cycles.

Figure 12: Comp B ATC07-3- A46

Figure 13: Comp B ATC09-4-BF46

The onset of failure occurs slightly earlier in the FR devices than in the PA lot but the distributions terminate similarly and can be combined into a single distribution. These distributions and the associated 90% CC are displayed in Figure 14 and Figure 15 respectively. This is also typical for this type of device. The extended reflow time produced by the more limited heat transfer available from hot gas rework equipment and the different temperature distribution across the device result in a lower average standoff height for FR devices Table 10 which accounts for this minor difference in the onset of failure.

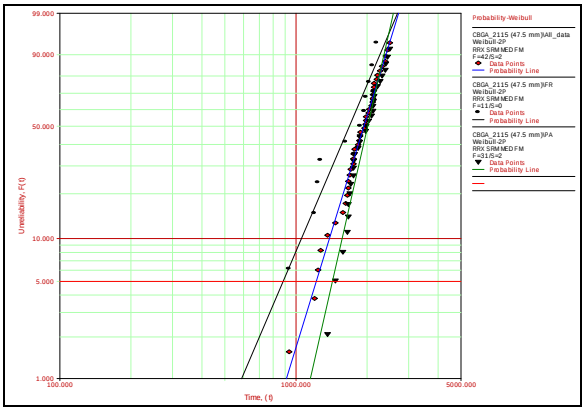

Figure 14: Comp B Weibull Distributions

Figure 15: Comp B, 90% CC

This combined distribution produces a nominal B4% value of 1170 cycles which is relatively consistent with other testing performed on these LTCC substrates on smaller devices by Butel [4].

Table 10: Comp B - Solder Joint Height (um)

SN- Ref lot	A46	M35	AC24	AR12	BF1	Delta
ATC12-1 PA	376.03	395.15	392.60	387.51	360.73	34.42
ATC12-4 FR	359.51	364.55	354.36	356.91	359.46	10.19

COMPONENT C

The Weibull distributions for component C are interesting because they demonstrate the separation of component package construction and Level 2 solder fatigue generated by the LTCC substrates. Figure 16 and Figure 17 demonstrate that there is no statistically significant difference between any of the lid or lid attach materials. We

should note that choosing the wrong materials for lid/attach can induce package level failures.

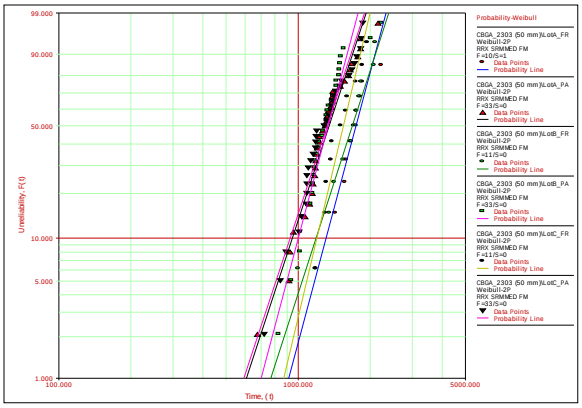

Figure 16: Comp C Weibull Distributions

Once again the stress concentration induced by the larger DNP and the implementation of SMD pads at the corners produces recrystallization and crack coalescence in the bulk solder near the top of the board level solder mask. Figure 18 and Figure 19 exhibit these effects at the A48 position of a FR component that was identified as a resistance failure at 1185 cycles and removed for destructive analysis at 1652 cycles. The B4% value for the entire 132 components in this project was 850 cycles.

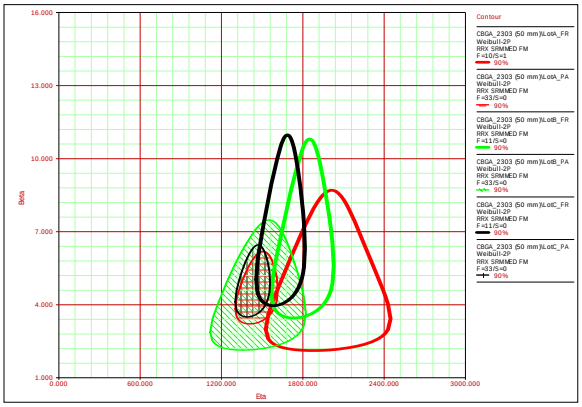

Figure 17: Comp C – 90% CC

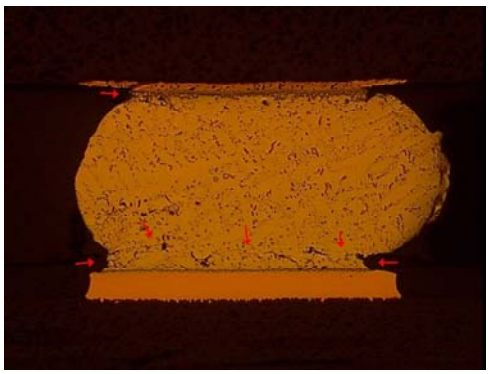

Figure 18: ATC34-4-A48 Solder Joint

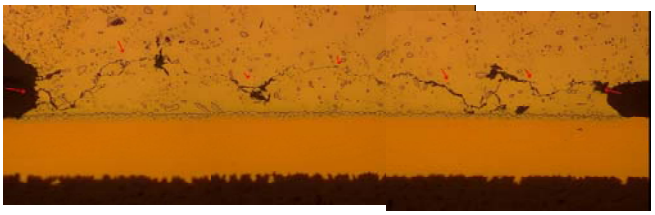

Figure 19: ATC34-4-A48 Crack Path

COMPONENT B – EDGE BOND

In preparation for the testing, a dispensing process was developed to generate a consistent edge bond fillet which did not fully involve any of the solder joints on the component. In the end, the rheology of the material and the design of the component made this impossible. There is no process which would not fully surround the corner sphere of the device. Looking forward, a simple depopulation of the corner sphere would make that goal achievable if required. The parts are fully reworkable with the current edge bond dispense process. Figure 20 exhibits the board edge bond interface and the detailed view of the corner solder sphere.

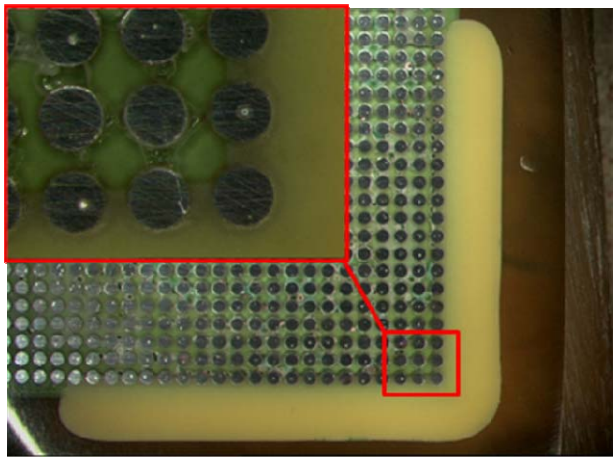

Figure 20: Edge Bond Flat Section

The edge bonded lot of component B consisted of 24 parts and was terminated at 3517 ATC cycles. All of the monitored channels passed electrical testing to that point. This provided us with the information that first failure and the B4% value are both greater than 3517.

This increase in chamber life has two primary causes. The reduced stress caused by the bonding of the component body to the board surface except for short spaces at the center of the device and the effective reduction in DNP from the diagonal distance to the rectangular distance from center to edge.

Post cycling, two samples were sent for destructive failure analysis. One component was processed through Dye penetration analysis and another through X-sectioning.. The dye and pry results looked excellent, with very little dye penetration near two of the four corners on the board side of the bulk solder. The cross section results along column 46 exhibited the onset of solder fatigue damage at the corners

of the device near the top of the solder mask in the SMD pads. However there was more extensive fatigue damage visible at the center of the component edge in the bulk solder on the component side as shown in Figure 21. The solder joints with fatigue damage are identified with red arrows and coincide with the gap in the edge bond material. The limit of the edge bond material is highlighted by the yellow arrows. The extent of the damage visible in Figure 22 is typical and suggests that electrical resistance failure was probable in the next few hundred cycles if stressing had continued.

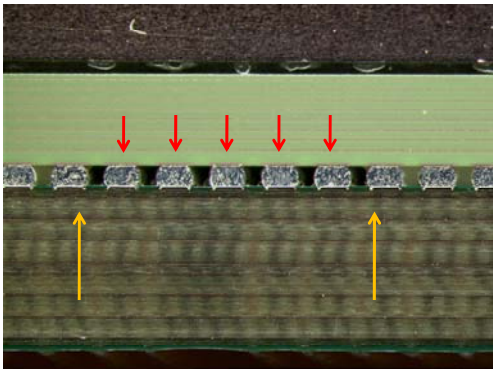

Figure 21: Edge Bond vertical section Col 46

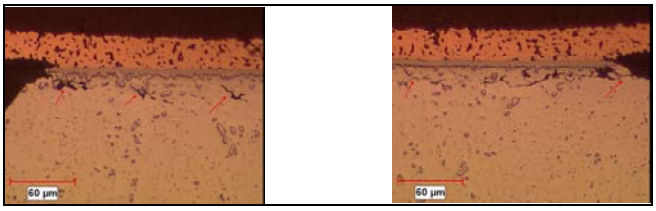

Figure 22: Comp B EB01-3-AA46

COMPONENT D

Primary attach solder heights were not apparently affected by the placement of the 0402 package under the corners of the component. The CBGA device was not in contact with the resistors in the as soldered condition. However, Table 11 displays that the average height of the FR lot is more similar to the PA lot than previous experience would predict. There is an apparent beneficial contact under extended reflow as would be expected. Commercial parts are now available as alternatives to the use of 0402 packages.

Table 11: Comp D - Solder Joint Height (um)

SN- Ref. Lot	C3	R15	AG27	AW39	BM52	Delta
ATC012-1 PA	409.1	400.1	382.3	397.6	410.3	28.0
ATC012-4, FR	407.8	402.7	410.0	420.5	402.3	18.2

The Edge Bond interface with the board is displayed by flat section in Figure 23 which shows that there are no fully encircled solder joints when the corner of the array is depopulated.

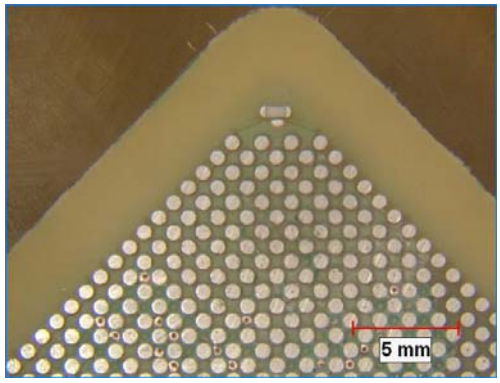

Figure 23: Comp D Flat section

All 44 monitored devices remained below the electrical resistance criteria when the chamber cycling was terminated at 3010 cycles. Post cycling, components were cross sectioned at the outside row. Figure 24 displays the solder joints at locations A25 and A28 of the ATC05-2 device which were typical of the damage accumulated in the unsupported area of the outside rows of these components at 3010 cycles.

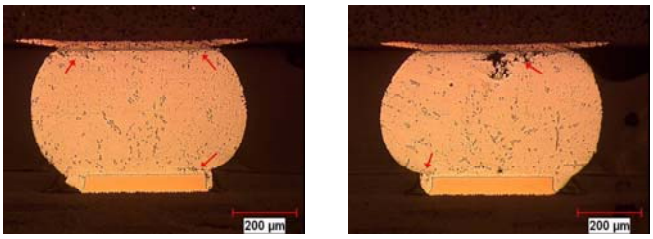

Figure 24: ATC05 A25 & A28 - 3010 cycles.

DISCUSSION

Across all of the five projects there were several constant factors. Laminate material and therefore T_g, T_d & CTE at the board level are constant. Solder sphere alloy and solder paste alloy for every test was SAC305. All components were processed with no clean ROL0 flux systems. Component ball pitch and solder sphere size were also constant across all of the projects.

Inspection of Table 12 reveals that board thickness, layer count and component substrate material were consistent across four of the five projects. We have included information on die size but the fact that solder fatigue is always directly relatable to DNP of the substrate suggests that this is not an important parameter.

Table 12: Parameter Summary

Comp.	A	B	B-EB	C	D
TV Layers	12	16	16	16	16
TV (mm)	2.34	3.175	3.175	3.175	3.175
Corner Pads	NSMD	SMD	SMD	SMD	NSMD
Body (mm)	32.5	47.5	47.5	50	55
DNP (mm)	21.6	32.9	32.9	34.3	37.8
IO	937	2115	2115	2303	2892
Die (mm^2)	~100	420	420	324	676
Substrate	Al_2O_3	LTCC	LTCC	LTCC	LTCC
Edge Bond	==	==	EB	==	EB
Eta	327	2072	==	1513	==
Beta	9.78	5.602	==	5.547	==
B4%	236 ?	1170	> 3517	850	> 3010

There was some discussion in 2005 about whether the life times predicted for Component A were real. Previous testing that utilized larger board side pads and larger spheres had produced Eta values near 700 cycles. Our assignment of the reduction in cycling life to the solder volume and pad configuration may be misplaced. But even if the B4% value of 236 underestimates this component by 100% the improvement based on moving to an LTCC substrate is substantial. Comparison of the parameters and results associated with the A & B components indicates that even though there is a higher driving force from the board stack and a larger DNP in the component B testing, it is more than compensated for by the increase in substrate CTE. The increase in B4% value from 235-500 to 1170 represents a 2.5X to 4.95X increase in cycling life.

Comparison of the results associated with the B & C components leads directly to the requirement for some enhancement to standard solder attachment. The reduction in B4% value from 1170 to 850 appears to be related directly to DNP.

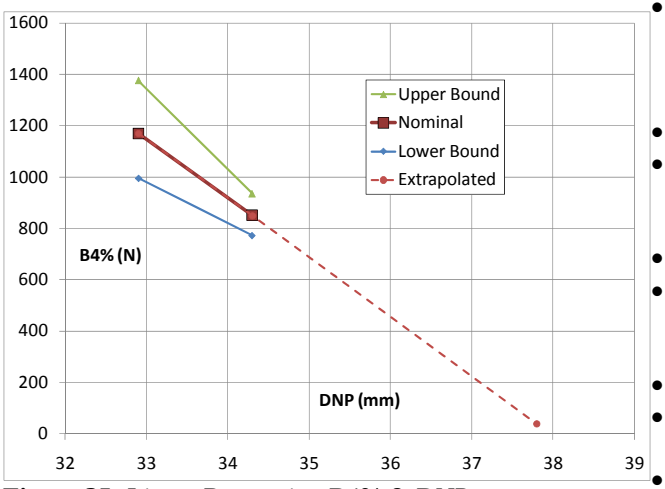

Figure 25: Linear Regression B4% & DNP

The internal component structures were unknown and the only real difference on the board side was the removal of SMD pads at the corners of the C component. One would expect the pad change to improve cycling performance rather than reduce it. This B4% reduction of 30% based on the increase of DNP from 32.9 mm to 34.5 mm and the increasing mass of the component would lead one to predict a B4% below 50 cycles for a 55 mm component with a DNP of 37.8 mm assuming a linear relationship as depicted in Figure 25.

The edge bonded version of component B did not fail in cycling before the test was terminated however for a lot of 24 a single failure represents 4.25% of the population. Since we have no failures we can only say that the B4% value is greater than the 3517 cycles at this test condition. This 3X improvement over the unsupported component is graphically represented in Figure 26.

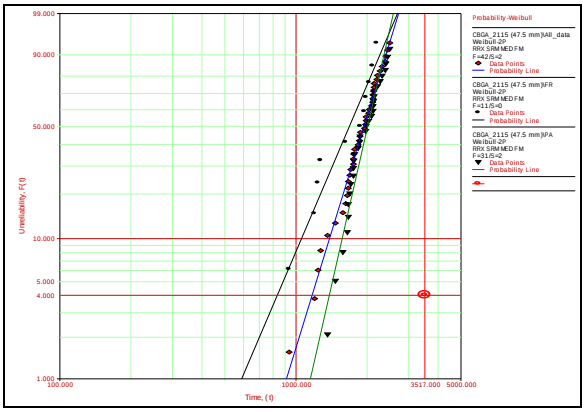

Figure 26: Comp B: Edge Bond Cycling Improvement

The subsequent cycling of 44 pieces of the 55 mm component to 3010 cycles without an electrical resistance failure indicates a similar or better improvement in chamber cycling lifetime for that larger package.

CONCLUSIONS

These observations lead us to the following conclusions:

The use of SMD pads at the corners of Ceramic parts for mechanical support can affect the region of solder fatigue within the BGA solder joint but does not appear to have any significant impact on chamber life.

The beneficial effect of LTCC substrate material is significant and has by itself extended the chamber life of ceramic components.

The use of standoffs under the corners of large ceramic BGA packages appears to generate more consistent solder joint heights from PA and FR processes.

The use of modern edge bond material can significantly increase chamber cycling life by a factor of 3X or more.

The positive effect of edge bond material has been replicated in multiple ATC tests using IPC9701, Test Condition 1.

ACKNOWLEDGMENTS

The authors would like to acknowledge Indium Corp. and Zymet Adhesives & Encapsulants for their contributions of material.

REFERENCES

1. IPC/JEDEC – 9701, Performance Test Methods and Qualification Requirements for Surface Mount Solder Attachments.
2. Song F., Yang, C., Effects of Corner and Edge Bond Epoxy adhesives on Board level solder Joint Reliability of BGA Mezzanine Connectors. ECTC 60, June 2010
3. Cole M. et al, Reliability Study and Solder Joint Microstructure of Various SnAgCu Ceramic Ball Grid Array Geometries and Alloys. SMTAI 2006.
4. Butel N., Comparison of the Level 2 Characteristics of HITCE Substrate assembled with SAC and High Lead Balls, SMTAI 2007.